Detection of caustics and interpolation of later-arrival traveltimes

C. Vanelle, J. Dettmer, and D. Gajewski

email: *vanelle@dkrz.de*

keywords: *Traveltimes, Interpolation, Kirchhoff Migration, Caustics*

ABSTRACT

Interpolation of seismic traveltimes plays an important role for many applications. However, interpolation schemes based on a local approximation of the traveltime functions fail in the presence of later arrivals and triplications of the wavefronts. In this paper we suggest a method to locate triplications and correctly interpolate first and later-arrival traveltimes using a hyperbolic traveltime expression.

INTRODUCTION

Multi-arrival traveltimes are important for a variety of applications, e.g., for migration. Due to the high demands in computational storage it is common to apply traveltime interpolation onto the fine migration grid. An efficient and accurate interpolation method can lead to a significant reduction of computer storage. However, interpolation schemes based on a local approximation of the wavefronts fail in caustic regions, as shown in our examples below (Figures 8–10, left). Except for the regions surrounding the discontinuities in the wavefronts the errors of the interpolation are very small. The high errors near the discontinuities are caused by the fact that local interpolation schemes usually approximate the wavefronts with smooth functions. Therefore, they fail in the vicinity of discontinuous wavefronts.

METHOD

The hyperbolic traveltime formula

The method is based on the hyperbolic traveltime expansion described in Vanelle and Gajewski (2002), which uses the Taylor expansion of the squared traveltime, T^2, near a receiver at $\mathbf{g}_0$. It leads to

$$T^2(\mathbf{g}) = (T_0 + \mathbf{q}\,\triangle\mathbf{g})^2 \;+\; T_0\,\triangle\mathbf{g}^\top\,\underline{\mathsf{G}}\,\triangle\mathbf{g} \quad , \tag{1}$$

introducing the slowness vector $\mathbf{q}$ and the second-order derivative matrix $\underline{\mathsf{G}}$,

$$\mathbf{q} = \boldsymbol{\nabla} T \qquad \text{and} \qquad \underline{\mathsf{G}}_{ij} = \frac{\partial^2 T}{\partial g_i\,\partial g_j} \quad .$$

If the coefficients T_0, $\mathbf{q}$, $\underline{\mathsf{G}}$ are known for a position $\mathbf{g}_0$, they can be used to interpolate traveltimes in the vicinity of $\mathbf{g}_0$ using Equation (1). Let traveltimes be given on coarse grids. These can be used to determine the coefficients of (1) and then carry out traveltime interpolation onto a finer grid. The coefficients of a variant of the hyperbolic equation including source terms (Vanelle and Gajewski, 2002) can also be used to compute weight functions for amplitude-preserving migration (Gajewski and Vanelle, 2002).

Determination of the coefficients

Consider the traveltime T_0 from a source at the position $\mathbf{s}_0$ to a receiver at $\mathbf{g}_0$ as expansion point and the traveltimes T_1 and T_2 which lie on the coarse grid positions adjoining $\mathbf{g}_0$ at $\mathbf{g}_0 \pm \triangle g_x$ (see Figure 1). The

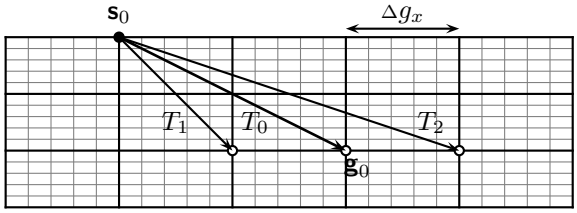

Figure 1: Traveltimes T_0, T_1, T_2 on the coarse grid with spacing Δg_x.

traveltimes T_1 and T_2 are substituted into the hyperbolic expression (1):

$$\begin{aligned} T_1^2 &= (T_0 - q_x\,\Delta g_x)^2 + T_0\,G_{xx}\,\Delta g_x^2 \\ T_2^2 &= (T_0 + q_x\,\Delta g_x)^2 + T_0\,G_{xx}\,\Delta g_x^2 \end{aligned}$$

This resulting system of equations is solved for the two unknowns q_x and G_{xx}:

$$q_x = \frac{T_2^2 - T_1^2}{4\,T_0\,\Delta g_x} \qquad \text{and} \qquad G_{xx} = \frac{T_2^2 + T_1^2 - 2\,T_0^2}{2\,T_0\,\Delta g_x^2} - \frac{q_x^2}{T_0}$$

The coefficients q_z and G_{zz} are determined accordingly from traveltimes to $\mathbf{g}_0 \pm\Delta g_z$ and so forth.

Traveltime interpolation

With all coefficients of (1) determined, the interpolation onto the fine grid can be carried out, as shown in Figure 2.

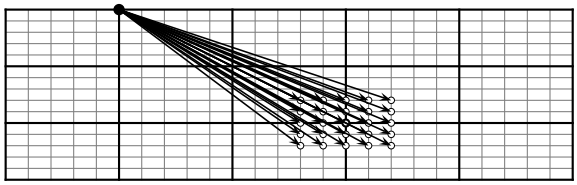

Figure 2: Interpolation of traveltimes onto the fine grid. The high accuracy and efficiency of the hyperbolic interpolation method was in detail investigated by Vanelle and Gajewski (2002). Examples including complex 3D models and interpolation of the source position can also be found there.

Discontinuities in the first arrival traveltimes

Equation (1) requires continuity of first- and second-order traveltime derivatives. This is apparently not fulfilled for first arrivals in the vicinity of a triplicated wavefront. Therefore the determination of the coefficients, and thus the traveltime interpolation fails, as displayed in Figure 3. The coefficients at both coarse grid points that frame the discontinuity, and therefore the interpolated traveltimes in the region surrounding them are affected.

The problems in caustic regions are not restricted to the hyperbolic expression but occur with every interpolation scheme based on a local approximation. To correctly deal with these regions, the traveltime branches left and right of the discontinuity need to be treated individually, e.g. by extrapolation from unaffected coefficients, as Figure 4 demonstrates.

In conclusion, to obtain better traveltimes in the vicinity of a discontinuity, we must

- locate the position of the discontinuity (denoted by P, see Figure 7),
- extrapolate traveltimes onto the fine grid from both sides until P using the nearest unaffected coefficients.

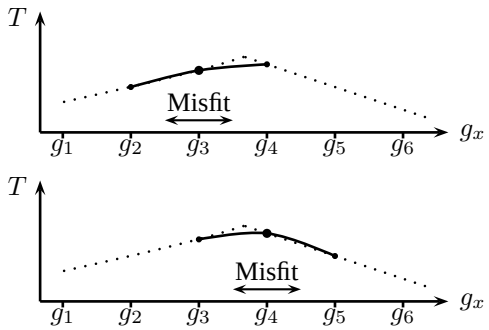

Figure 3: Traveltime curve (dotted line) and hyperbolic approximation (solid line). Coefficients computed from traveltime values at both sides of a discontinuity lead to a misfit between $g_3 - \Delta g_x/2$ and $g_4 + \Delta g_x/2$.

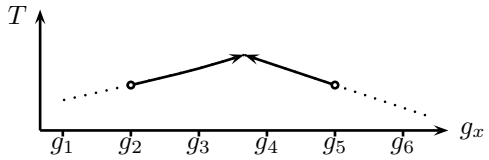

Figure 4: The coefficients at grid points g_3 and g_4 are wrong. Better fitting traveltimes can be obtained by extrapolation from g_2 and g_5.

Discontinuities and multi-arrival traveltimes

If multi-arrival traveltimes are available, they can be interpolated individually with a set of coefficients at each coarse grid point for each arrival. However, we encounter a similar problem as for the use of first-arrival traveltimes only: near a triplication of the wavefront we need to decide on the appropriate combination of first- and second-arrival traveltimes for the computation of the coefficients (see Figure 5). This combination depends on the position of the discontinuity.

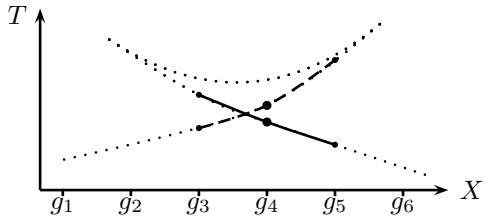

Figure 5: First-, second-, and third-arrival traveltimes. The correct coefficients, here for the first (solid line) and second (dashed line) arrivals at g_4, can be obtained from combining the appropriate traveltimes as shown.

Here the strategy to correct the traveltimes is to

- locate the position of the discontinuity,
- correct the coefficients,
- interpolate the left and right branches separately for first and later arrivals.

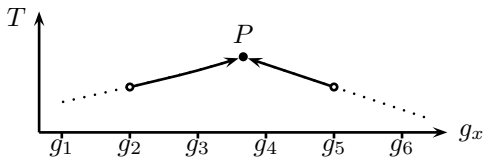

Figure 6: The coefficients at grid points g_3 and g_4 are wrong. Traveltimes are extrapolated from g_2 and g_5. They intersect at P, the location of the discontinuity.

Locating discontinuities

A discontinuity leads to a negative value of the coefficient G_{xx} for the first-arrival traveltimes at the two coarse grid points which frame it (Figure 4). To detect a discontinuity we search for grid points where G_{xx} is significantly more negative than in their surroundings. We then extrapolate the traveltimes from the next unaffected grid points on the left and right towards the discontinuity and solve for the intersection point P, as shown in Fiure 6. The coefficients G_{zz} are investigated accordingly.

EXAMPLES

Detection of discontinuities

In this first example we demonstrate the detection of discontinuities in the first-arrival traveltimes. Traveltimes were generated on a coarse grid with 100 m spacing using the wavefront oriented ray tracing technique (Coman and Gajewski, 2001) for a model with a low velocity lens. The discontinuities were detected as described above, by first selecting coarse grid points with negative G_{xx} followed by extrapolation from uncontaminated grid points and solving for P, the location of the discontinuity. Figure 7 demonstrates the reliability of the detection.

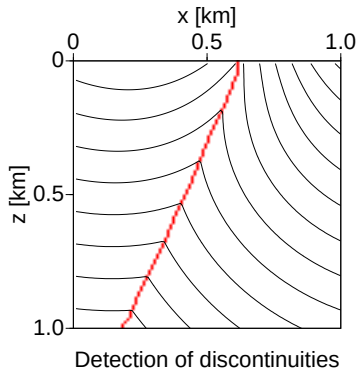

Figure 7: Detection of discontinuities: isochrones and the detected locations P on the fine grid. The mismatch between the real and detected position near $z = 0$ is a border effect.

Extrapolation of first-arrival traveltimes

In this example we have used first arrival traveltimes only. The coefficients were determined and the traveltimes interpolated onto a fine 10 m grid. In regions with discontinuous wavefronts, the discontinuities were detected and traveltimes were extrapolated from uncontaminated grid points. The resulting relative errors are shown in Figure 8. Whereas the mean error for the traveltimes from the original hyperbolic interpolation without considering the discontinuities is 0.113 %, the error was reduced to 0.014 % by the extrapolation in the affected region.

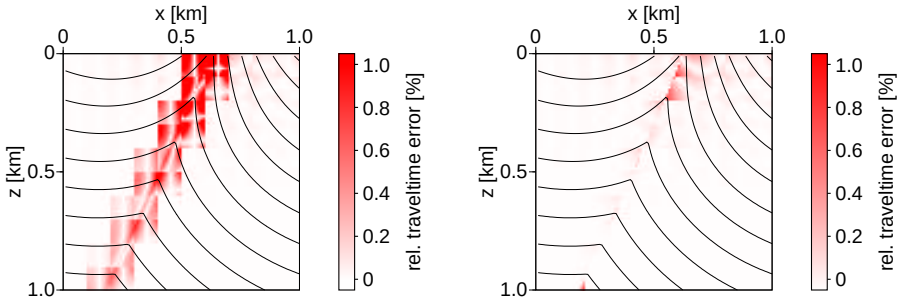

Figure 8: Extrapolation of first-arrival traveltimes. Left: only hyperbolic interpolation was carried out. On the right the traveltimes in the region surrounding the discontinuity were corrected by extrapolation from unaffected grid points. This technique of traveltime extrapolation can also be applied in combination with multi-arrivals, e.g., in regions where a caustic begins to form and later arrivals are not yet available for all of those coarse grid positions where they are needed for the determination of the coefficients.

Interpolation of multi-arrival traveltimes

This example shows how the accuracy of the interpolation of first and second arrivals is enhanced by our technique. Third and later arrivals can be treated accordingly. Hyperbolic traveltime interpolation was carried out using the uncorrected coefficients for first and second arrivals. The resulting relative errors are shown in the left part of Figure 9 for the first arrivals, and Figure 10 for the second arrivals. Then the discontinuities were detected and the coefficients were corrected for both first and second arrivals. Traveltimes were interpolated onto the fine grid using the appropriate coefficients for each fine grid point. The results are shown in Figures 9 and 10 (right). For the first arrivals the mean error was reduced to 0.014 %, as in the case of extrapolation. For the second arrivals the mean error was reduced from 0.249 % in the uncorrected version to 0.006 %.

As already indicated, we can combine the extrapolation technique with the interpolation using corrected coefficients in regions where the triplications form.

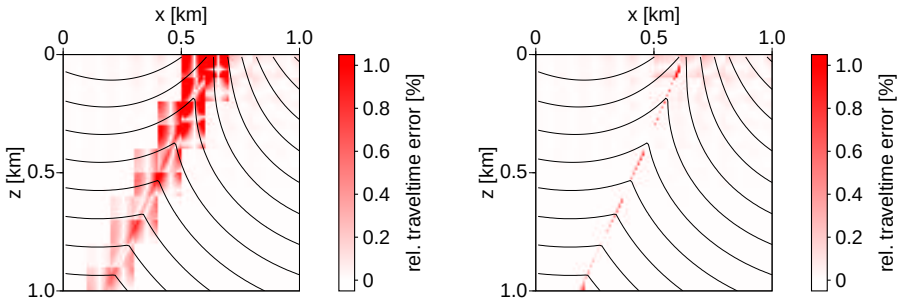

Figure 9: Interpolation of first-arrival traveltimes. Left: without accounting for discontinuities, right: with corrected coefficients using first and second-arrivals traveltimes.

CONCLUSIONS AND OUTLOOK

We have introduced a method to detect caustics and regions with discontinuous wavefronts. With this information we can correctly handle the traveltime branches and thus overcome the problems related to local traveltime approximations in the vicinity of discontinuous wavefronts. We have shown in a simple example that the errors can be reduced by a magnitude with our technique. Investigations carried out by Dettmer (2002) show that the method performs equally well in 3D. In this case, however, we must take care to distinguish between line foci and point foci (Figure 11).

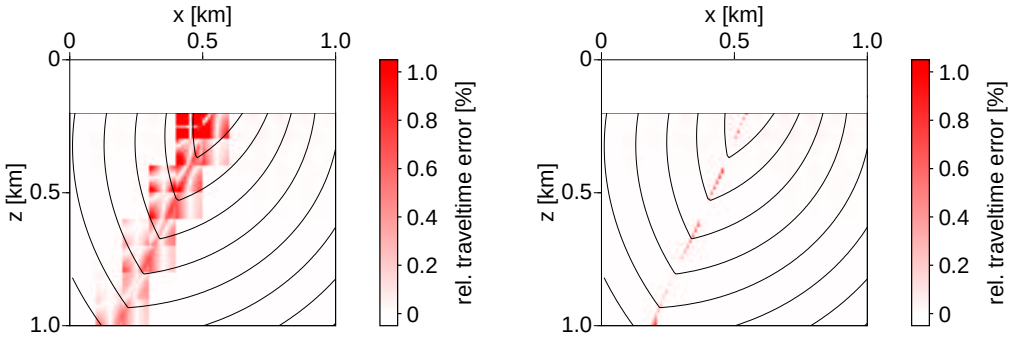

Figure 10: Interpolation of second-arrival traveltimes. Left: without accounting for discontinuities, right: with corrected coefficients.

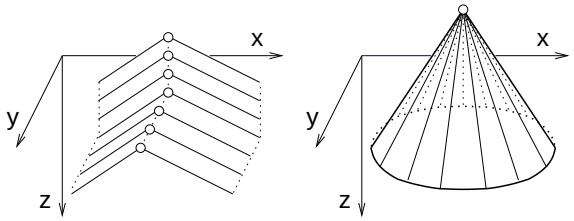

Figure 11: First-arrival wavefronts forming a line focus (left) and a point focus (right). The circles indicate the locations of the discontinuities.

We are currently working on an implementation that also considers discontinuities for the interpolation of the source position (Vanelle and Gajewski, 2002). Since the coefficients involved in the corresponding expression can be used to compute geometrical spreading from traveltimes (Vanelle and Gajewski, 2003), this extension will also lead to more accurate geometrical spreading in regions with discontinuous wavefronts. The geometrical spreading is a key ingredient to compute true-amplitude migration weight functions. Here, later arrivals are crucial for the imaging of complex structures (Geoltrain and Brac, 1993). Pending further investigation this will make the method particularly suited for an application within the traveltime-based strategy for amplitude-preserving migration (Gajewski and Vanelle, 2002).

ACKNOWLEDGEMENTS

We thank the members of the Applied Geophysics Group in Hamburg for continuous discussions. Radu Coman provided the 2-D wavefront ray tracing code and thus the necessary input traveltimes. This work was partially supported by the sponsors of the Wave Inversion Technology (WIT) Consortium and the German Research Foundation (DFG, grants Ga 350/10-1 and Va 207/2-1).

REFERENCES

Coman, R. and Gajewski, D. (2001). Estimation of multivalued arrivals in 3-D models using wavefront ray tracing. In *Expanded Abstracts*. Soc. Expl. Geophys.

Dettmer, J. (2002). Traveltime interpolation in caustic regions (in German). Master's thesis, University of Hamburg.

Gajewski, D., Coman, R., and Vanelle, C. (2002). Amplitude-preserving Kirchhoff migration – a traveltime-based strategy. *Studia geophysica et geodaetica*, 46:193–211.

Geoltrain, S. and Brac, J. (1993). Can we image complex structures with first arrival traveltime? *Geophysics*, 58:564–575.

Vanelle, C. and Gajewski, D. (2002). Second-order interpolation of traveltimes. *Geophysical Prospecting*, 50:73–83.

Vanelle, C. and Gajewski, D. (2003). Determination of geometrical spreading from traveltimes. *Journal of Applied Geophysics (in press)*.